Supporting Information for

Luciferase activity of insect fatty acyl-CoA synthetases with synthetic luciferins

David M. Mofford, Kate L. Liebmann, Ganapathy Subramanian Sankaran, G.S. Kiran Kumar Reddy, G. Randheer Reddy, Stephen C. Miller*

Department of Biochemistry and Molecular Pharmacology, University of Massachusetts Medical School, Worcester, MA, 01605, United States

Table of Contents

Supplementary Methods:

General

NMR spectra were acquired on a Bruker Avance III HD 500 MHz. High-resolution mass spectra (HRMS) were recorded at the UMass Mass Spectrometry Facility on a Thermo Scientific Orbitrap Velos Pro mass spectrometer coupled with a Thermo Scientific Accela 1250 UPLC and an autosampler using electrospray ionization (ESI) in the positive mode. HPLC purification was performed on an Agilent 1100 using an Agilent 10 Prep–C18 250 x 21.2 mm column with linear gradient of 10% to 90% acetonitrile in H_2O over 40 min (flow rate 10 mL/min). A UV detector set at 330 nm was used for peak detection. GraphPad Prism ver. 7.0a (GraphPad Software, Inc.) was used to analyze data and generate graphs.

Enzyme Expression and Purification

CG6178, AbLL, and PaLL were codon-optimized for mammalian expression, synthesized by GenScript, and cloned into the BamHI–NotI sites of pGEX6P-1. Firefly luciferase and all ACSLs were expressed and purified as GST-fusion proteins in a pGEX6P-1 vector as previously described.[1] Briefly, JM109 cells were grown at 37 °C until the OD600 reached 0.5-1, induced with 0.1 mM IPTG, and incubated with shaking at 20 °C overnight. Cells were pelleted at 5000 rpm, then flash frozen in liquid nitrogen. The *E. coli* pellets from 1 L of culture were thawed on ice, resuspended in 25 mL lysis buffer (50 mM Tris [pH 7.4], 500 mM NaCl, and 0.5% Tween 20) containing 1 mM phenylmethylsulfonyl fluoride, and disrupted by sonification (Branson Sonifier). Dithiothreitol (DTT) was added at 10 mM, and the resulting cell lysate was clarified by ultracentrifugation at 35,000 rpm for 60 min at 4 °C. The supernatant was batch-bound to immobilized glutathione (Thermo Scientific) for 1 hr at 4 °C, and the beads were washed with lysis buffer containing 10 mM DTT, followed by wash buffer (50 mM Tris [pH 8.1], 250 mM NaCl, and 10 mM DTT) and enzyme storage buffer (50 mM Tris [pH 7.4], 0.1 mM EDTA, 150 mM

NaCl, 1 mM TCEP). Twenty units of PreScission Protease (GE Healthcare) were added, and incubation continued overnight at 4 °C to cleave the GST-fusion and elute the untagged enzyme. Protein concentrations were determined using Coomassie Plus (Thermo Scientific).

Burst Kinetics

For luciferin burst kinetics, 50 µL of each luciferin prepared at 500 µM in substrate buffer was added per well of a white 96-well plate (Costar 3912). For adenylate burst kinetics, 25 µL of D-luciferin, CycLuc2, or their respective adenylate prepared at 400 µM in 10 mM sodium acetate, pH 4.5 was added per well. Immediately prior to injection, 25 µL of adenylate burst buffer (40 mM Tris [pH 7.4], 0.2 mM EDTA, 16 mM $MgSO_4$) with 8 mM ATP for luciferins or without ATP for adenylates was added to each well. Using a Promega GloMax-Multi Detection System, 50 µL of purified enzyme in enzyme buffer was rapidly injected into each well to a final enzyme concentration of 100 nM for CG6178 and AbLL, 1 nM for FLuc with all synthetic luciferins, and 0.1 nM for FLuc with D-luciferin. Final substrate concentrations were 250 µM for luciferins and 100 µM for adenylates. Measurements were taken every 0.5 s for 1 s pre-injection and 120 s post-injection. Data are reported as Relative Light Units (RLU). FLuc data was corrected for enzyme concentration by multiplying the raw data by 1,000 for D-luciferin and its adenylate or by 100 for all other luciferins.

ATP Evaluation Assays Using Pyrophosphate and Pyrophosphatase

D-Luciferin and CycLuc2 were prepared at concentrations from 1,000 µM to 0.488 µM in evaluation buffer (20 mM Tris [pH 7.4] and 0.1 mM EDTA). ATP from either MP Biomedicals or Sigma Aldrich was prepared at 16 mM in evaluation buffer with 32 mM $MgSO_4$. Pyrophosphate was prepared at 1.6 mM, 160 µM, and 16 µM in evaluation buffer. Pyrophosphatase (NEB) was prepared at 4 units/mL in enzyme buffer. Luciferase and CG6178 were prepared at 80 nM in

enzyme buffer. In a black 96-well plate (Costar 3915), 25 µL luciferin, 12.5 µL ATP, and 12.5 µL pyrophosphate or evaluation buffer were added. Enzyme buffer (25 µL) was added, proceeding directly to luminescence, or pyrophosphatase (25 µL) was added and held at ambient temperature for 45 minutes. Luminescence was then initiated by adding 25 µL of luciferase or CG6178. Imaging was performed one minute after luciferase/CG6178 addition at final concentrations of 250 µM to 0.122 µM luciferin; 2 mM ATP; 0 µM, 2 µM, 20 µM, or 200 µM pyrophosphate; 0 or 0.1 units/well pyrophosphatase; and 20 nM luciferase/CG6178. Imaging was performed using a Xenogen IVIS-100. Data acquisition and analysis was performed with Living Image® software. Data are reported as total flux (p/s) for each ROI corresponding to each well of the 96-well plate.

Order-of-Addition Burst Kinetics

To each well of a white 96-well plate (Costar 3912), 50 µL of 2x enzyme in enzyme buffer was added. Immediately prior to injection, 25 µL of adenylate burst buffer (40 mM Tris [pH 7.4], 0.2 mM EDTA, 16 mM $MgSO_4$) with 8 mM ATP was added to each well. Using a Promega GloMax-Multi Detection System, 25 µL of 1,000 µM luciferin in evaluation buffer was rapidly injected into each well. Conversely, immediately prior to injection, 25 µL of 1,000 µM luciferin in evaluation buffer was added to each well. Adenylate burst buffer with 8 mM ATP (25 µL) was rapidly injected into each well. Final enzyme concentrations were 100 nM for CG6178 and AbLL, 1 nM for FLuc with CycLuc2, and 0.1 nM for FLuc with D-luciferin. Final luciferin substrate concentrations were 250 µM. Measurements were taken every 0.5 s for 1 s pre-injection and 120 s post-injection. Data are reported as Relative Light Units (RLU).

Circular Dichroism

Enzymes were prepared at 3 µM in enzyme storage buffer. Using a Jasco J-810 spectropolarimeter with a thermoelectric temperature control system, the native state circular

dichroism (CD) spectrum of each enzyme was collected from 260-205 nm in a 0.5 cm quartz cuvette at temperatures from 20-70°C, at 2°C intervals. Ellipticity (mDeg) at 222 nm was plotted as a function of temperature (°C) and fit to a sigmoidal dose-response curve by nonlinear regression to calculate the melting temperature of each enzyme. Data for each enzyme were normalized to 0% to 100% unfolded protein.

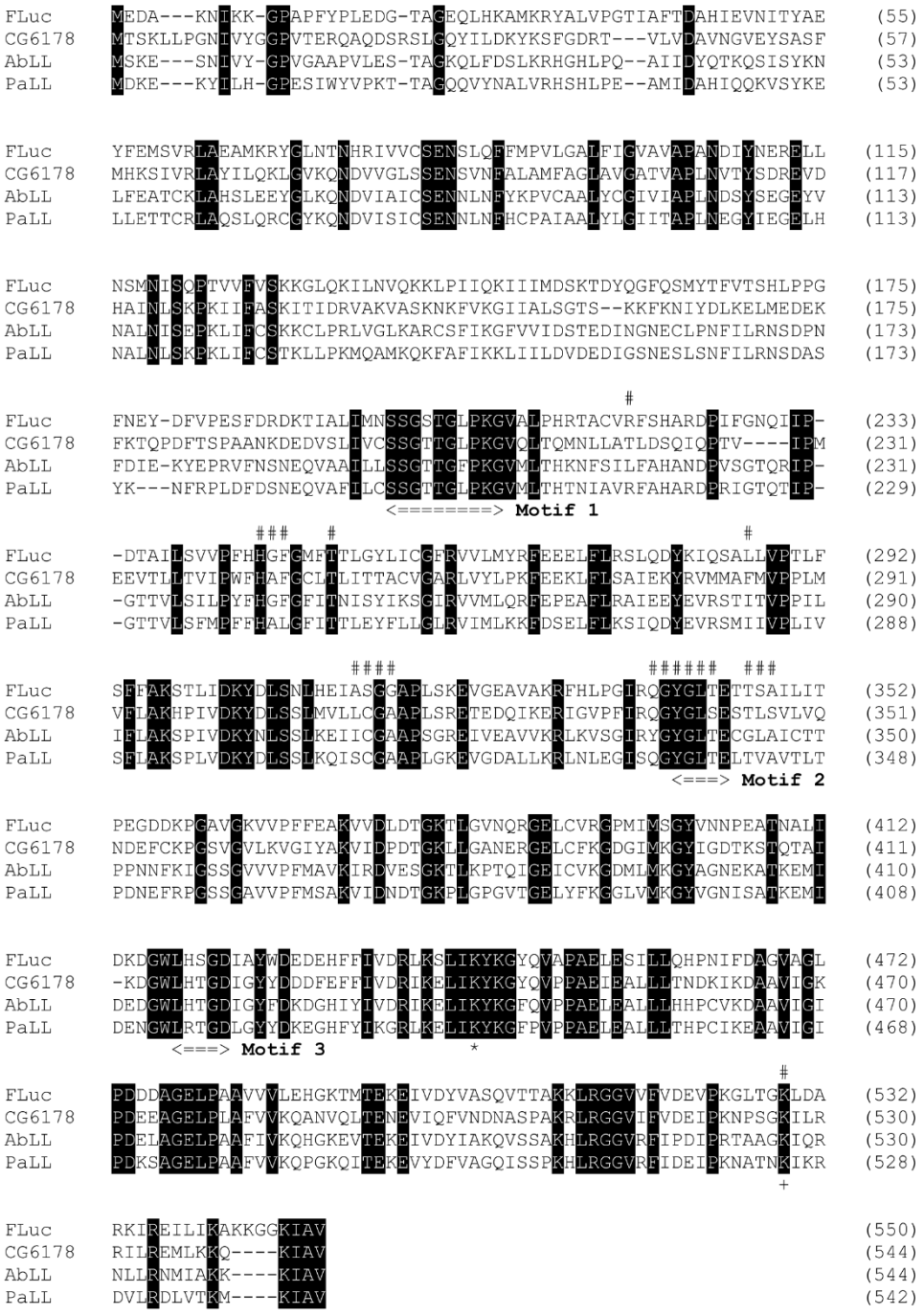

Figure S1. Primary sequence alignment of firefly luciferase and three fatty acyl-CoA synthetases. Primary sequences are displayed as a Clustal format alignment by Mafft [2]. Motifs 1-3 are conserved between members of the acyl-adenylate superfamily. Residues within 5 Å of the luciferin binding pocket are marked above with #. Luciferase K443 is involved in oxidation or thioesterification of the substrate and is marked below with *. Luciferase K529 is involved in adenylation of the substrate and is marked below with +.

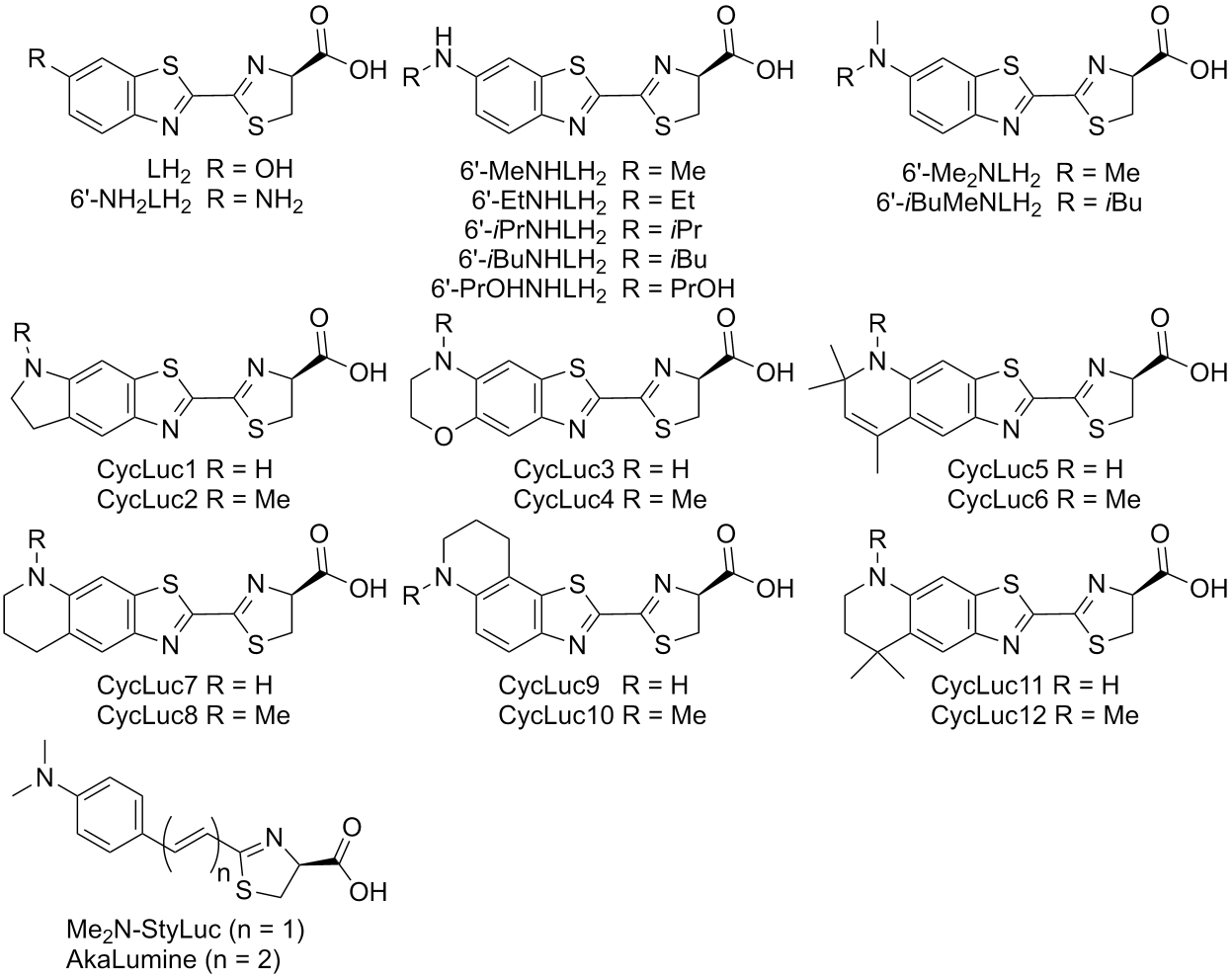

Figure S2. Chemical structures of luciferin substrates.

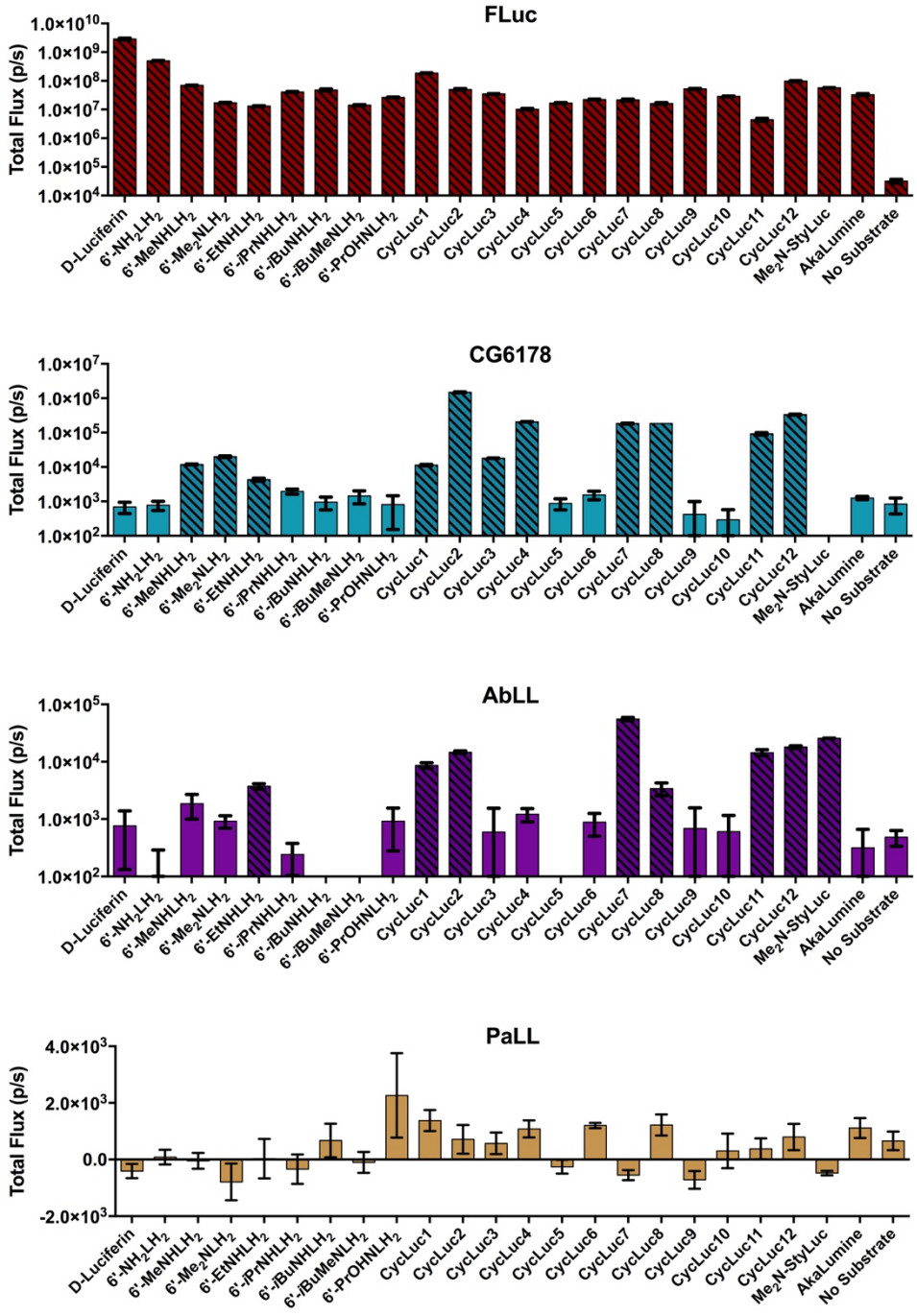

Figure S3. ACSL luciferase activity upon treatment with 250 μM of the indicated luciferin analog. The indicated ACSL (20 nM) was treated with the indicated luciferin analog (250 μM). The assay was performed in triplicate and is represented as the mean ± SEM. FLuc, CG6178, and AbLL are represented on a log scale. PaLL is represented on a linear scale. Each enzyme was compared by t test to a no substrate control. Striped bars show significant ($p < 0.05$) flux over no substrate. Solid bars are not statistically significant versus a no-substrate control.

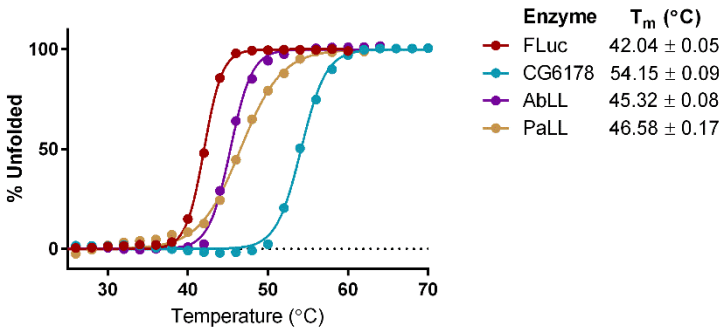

Figure S4. Thermal denaturation of each purified ACSL. Thermal denaturation profiles of each ACSL (3 μM) monitored by CD at 222 nm and normalized to % unfolded protein. The assay was performed in triplicate and is represented as the mean of three CD scans. Data were fit to a sigmoidal dose-response curve by nonlinear regression to calculate the melting temperature of each enzyme.

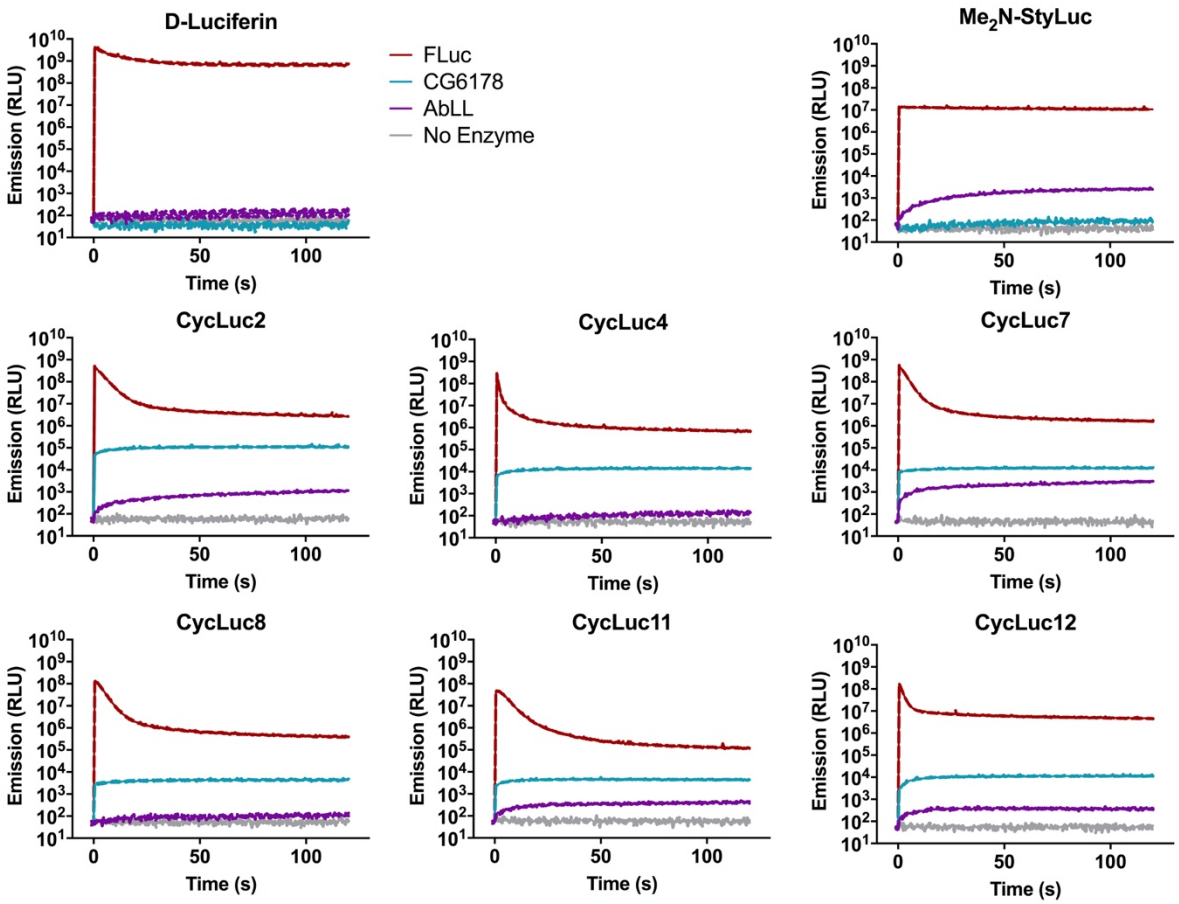

Figure S5. Burst kinetics of each ACSL with the indicated luciferin analog. Purified enzyme was rapidly injected into substrate (250 μM). Light emission was recorded every 0.5 s for 1 s pre-injection and 120 s post-injection. Background luminescent signal in the absence of enzyme is shown for reference (in gray). The assays were performed in triplicate, are represented as the mean ± SEM, and are presented on the same log scale.

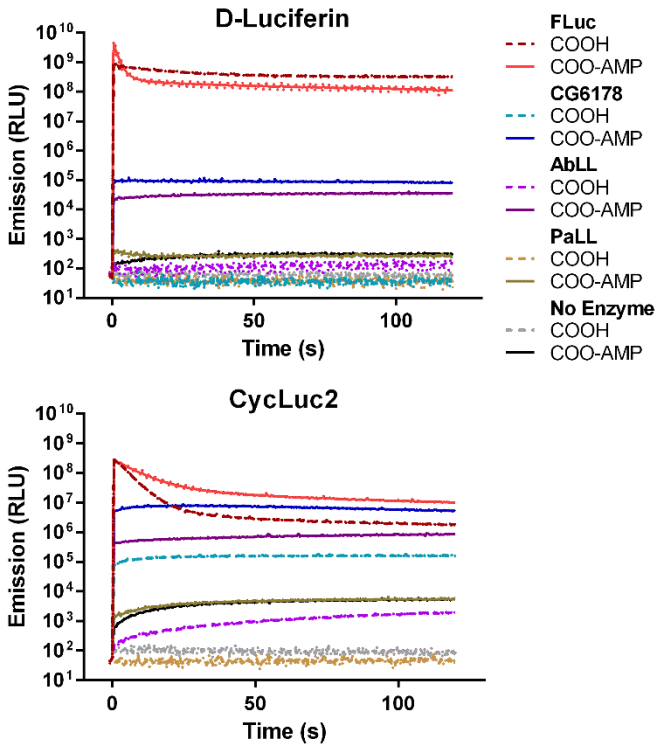

Figure S6. Burst kinetics profiles of FLuc and each ACSL with D-luciferin, CycLuc2, and their adenylates. Purified enzyme was rapidly injected into substrate (100 μM). Light emission was recorded every 0.5 s for 1 s pre-injection and 120 s post-injection. Background luminescent signal in the absence of enzyme is shown for reference (in gray). The assays were performed in triplicate, are represented as the mean ± SEM, and are presented on the same log scale.

Supplementary Discussion

While examining bioluminescence from the latent luciferases, we noticed a significant difference in photon flux with different brands of ATP. When using ATP purchased from Sigma Aldrich, bioluminescence from CG6178 and CycLuc2 was reduced by 13-fold compared to ATP from MP Biomedicals (**Figure S7**). We hypothesized that this difference was due to a small amount of contaminating pyrophosphate present in the ATP from Sigma. Consistent with this explanation, the deliberate addition of pyrophosphate to the MP Bio ATP resulted in a similar reduction of CG6178 bioluminescence (**Figure S8**). Moreover, pre-treatment of Sigma ATP with pyrophosphatase produced an increase in the bioluminescent signal, similar to that achieved with the MP Bio ATP (**Figure S8**). The contaminating pyrophosphate has the opposite effect on firefly luciferase, resulting in an almost three-fold increase in signal. Presumably this is due to reaction with the enzyme-bound potent inhibitor dehydroluciferyl adenylate to release dehydroluciferin and ATP.[3] Treatment of luciferase with high levels of pyrophosphate (200 μM; 10% of the ATP concentration), ultimately results in a lowered bioluminescent signal (**Figure S8**), consistent with previous observations.[3]

Light emission from CG6178 and AbLL as a function of luciferin concentration was poorly fit by a sigmoidal dose-response curve. However, the data fit well to a model for substrate inhibition (**Figure S7**). There are several mechanisms by which this could happen. The first and most trivial explanation is that the substrate nonspecifically interferes with enzyme activity at high concentrations (e.g., by denaturing the enzyme). Given the potency of these substrates, we find this mechanism unlikely. In a second and more selective explanation, substrate inhibition could be accounted for by an ancillary substrate binding site that allosterically reduces activity. Although substrate inhibition is more pronounced with the hydrophobic luciferins CycLuc11 and 12 that may be most prone to nonspecific binding to the enzyme, there is no obvious second binding site that would accommodate high-affinity binding to all of our luciferin analogs. Finally, in a third possibility, there could be a required order of binding for the two substrates. Fatty acyl-CoA synthetases are bisubstrate enzymes, where the carboxylate-containing substrate and ATP must both bind. If luciferin binding blocks subsequent ATP binding, no luciferase activity will be observed from that binding event and substrate inhibition by the luciferin would be observed. In this case, productive luciferase activity would require ATP to bind first, followed by the luciferin. However, initiation of bioluminescence by injection of either the luciferin or ATP (such that either ATP or the luciferin would be pre-bound to the enzyme) did not corroborate this model (**Figure S9**). The burst height of FLuc with both D-luciferin and CycLuc2 was slightly greater when the luciferin was injected into FLuc and ATP. Conversely, the AbLL burst height was slightly higher when ATP was injected, suggesting that luciferin pre-incubation does not impede ATP binding to AbLL. Finally, there was no difference in burst height with CG6178, suggesting that CG6178 does not have a preference in the order of binding. The root cause of the observed substrate inhibition thus remains unclear.

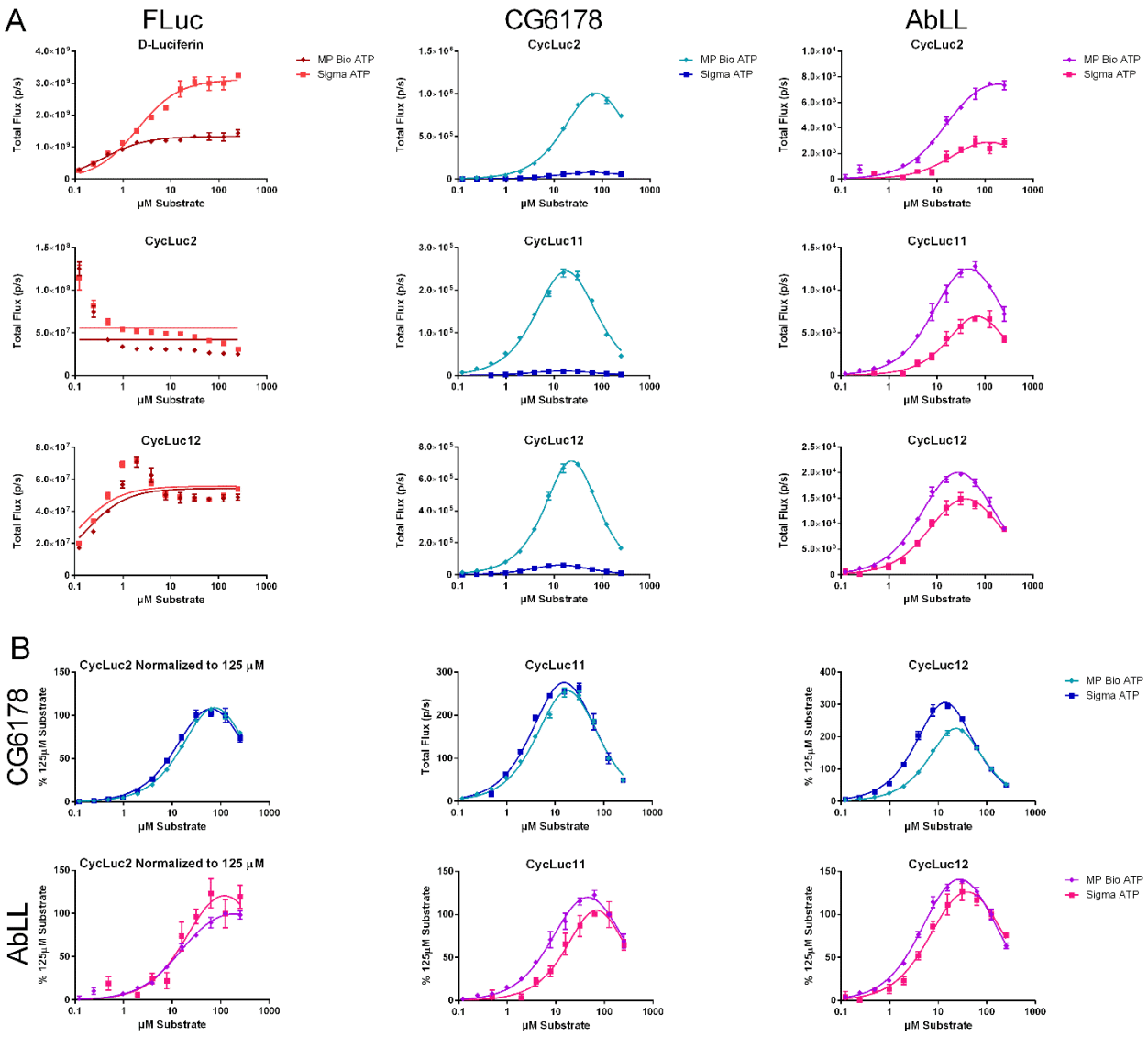

Figure S7. ATP purity affects ACSL luciferase activity. (A) Dose-response curves of indicated ACSL with indicated luciferin using ATP purchased from MP Biomedicals or Sigma Aldrich. (B) Dose-response curves of CG6178 and AbLL from (A) normalized to total flux at 125 μM substrate. The assays were performed in triplicate and are represented as the mean ± SEM. FLuc curves were fit to the Michaelis–Menten equation by nonlinear regression. CG6178 and AbLL curves were fit to the Substrate Inhibition equation [$Y=V_{max}*X/(K_m + X*(1+X/K_i))$] by nonlinear regression. Note: The Michaelis-Menten fits the FLuc data with CycLuc2 and CycLuc12 very poorly due to high levels of product inhibition.

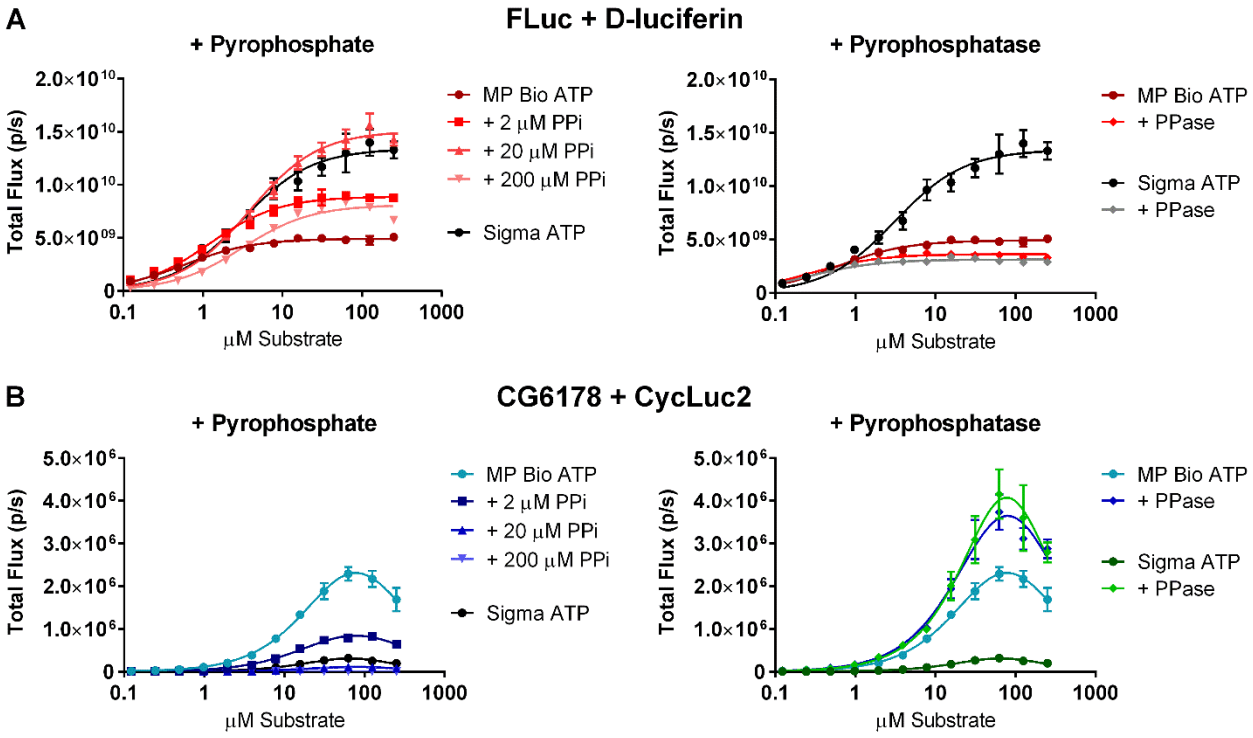

Figure S8. Pyrophosphate affects ACSL luciferase activity. Dose-response curves of (A) FLuc light emission with D-luciferin or (B) CG6178 light emission with CycLuc2 using ATP purchased from either MP Biomedicals or Sigma Aldrich. Left Panels: MP Bio ATP is supplemented with increasing concentrations of pyrophosphate (PPi). Right Panels: Each ATP with or without pre-treatment with pyrophosphatase (PPase). The assays were performed in triplicate and are represented as the mean ± SEM. FLuc curves were fit to the Michaelis–Menten equation by nonlinear regression. CG6178 and AbLL curves were fit to the Substrate Inhibition equation [$Y=V_{max}*X/(K_m + X*(1+X/K_i))$] by nonlinear regression. Note: Assays were run with 2 mM ATP final.

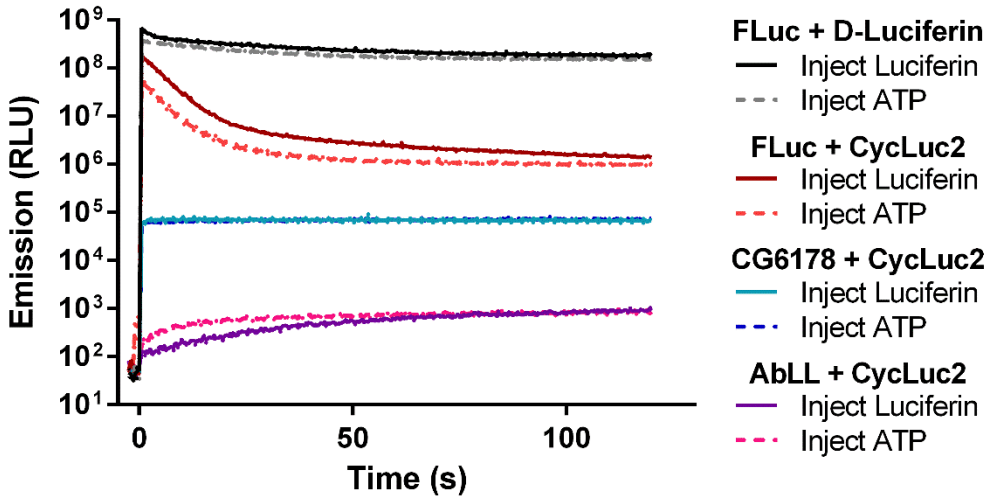

Figure S9. Substrate order-of-addition burst kinetics profiles of each ACSL with the indicated luciferin analog. Solid lines: Luciferin substrate (250 μM) was rapidly injected into purified enzyme (100 nM) pre-incubated with ATP (2 mM). Dashed lines: ATP substrate was rapidly injected into purified enzyme pre-incubated with luciferin. Light emission was recorded every 0.5 s for 1 s pre-injection and 120 s post-injection. The assays were performed in triplicate, are represented as the mean ± SEM.

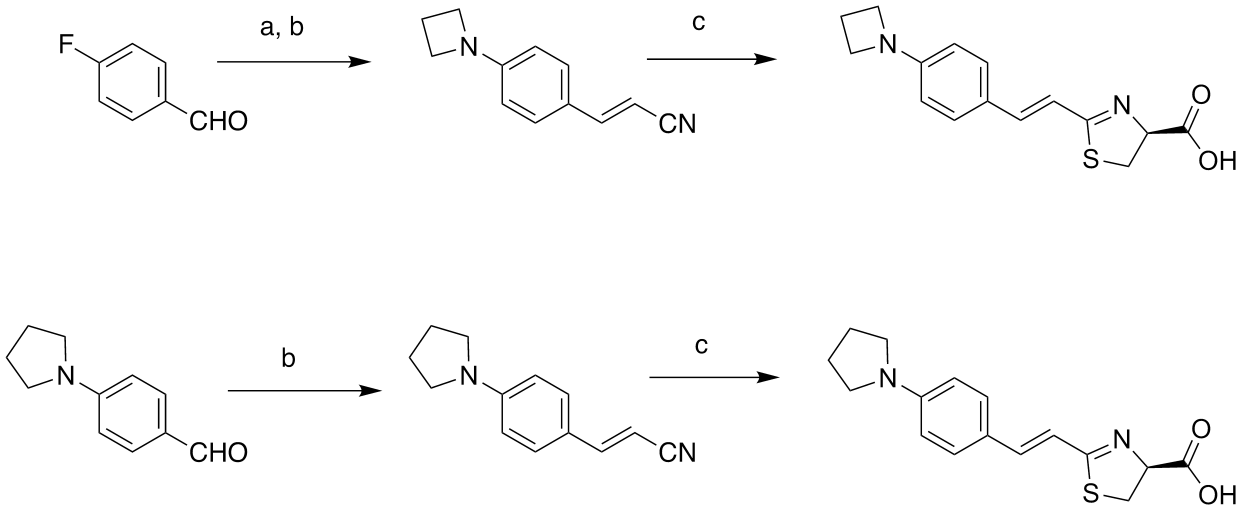

Scheme S1. Synthesis of Azet-StyLuc and Pyrr-StyLuc analogues**:** a) azetidine HCl, K_2CO_3, DMSO, 110 °C; b) diethyl cyanomethylphosphonate, NaH, THF, 0 °C; c) D-cysteine, aq alcohol, pH 8, 70 °C

Supplemental References:

(1) Mofford, D. M., Reddy, G. R., and Miller, S. C. (2014) Aminoluciferins extend firefly luciferase bioluminescence into the near-infrared and can be preferred substrates over D-luciferin. *J. Am. Chem. Soc. 136*, 13277–13282.
(2) Katoh, K., Misawa, K., Kuma, K., and Miyata, T. (2002) MAFFT: a novel method for rapid multiple sequence alignment based on fast Fourier transform. *Nucleic Acids Res. 30*, 3059–3066.
(3) Fontes, R., Fernandes, D., Peralta, F., Fraga, H., Maio, I., and Esteves da Silva, J. C. G. (2008) Pyrophosphate and tripolyphosphate affect firefly luciferase luminescence because they act as substrates and not as allosteric effectors. *FEBS J. 275*, 1500–1509.

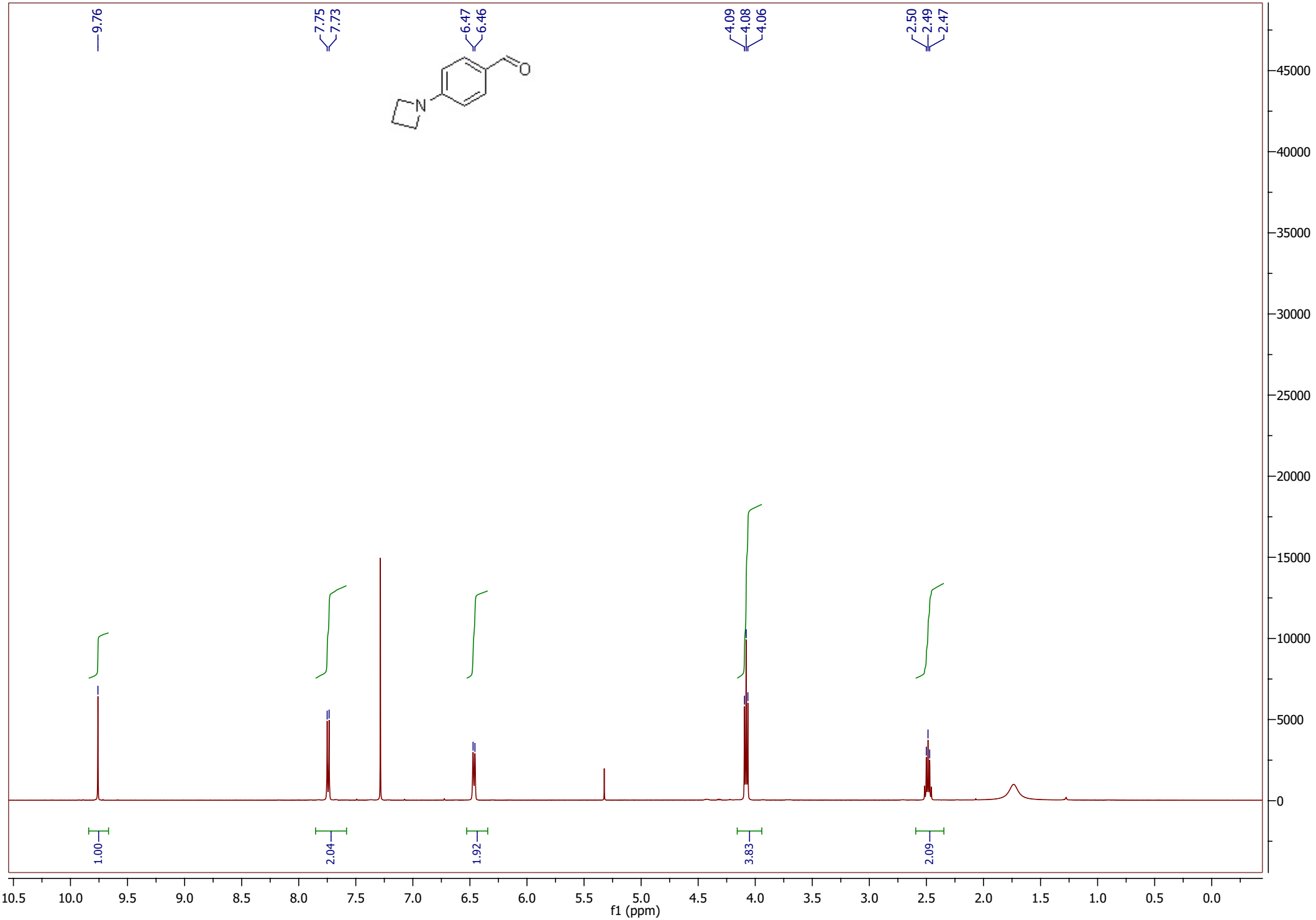
9.76
7.75
7.73
6.47
6.46
4.09
4.08
4.06
2.50
2.49
2.47
O
N
45000
40000
35000
30000
25000
20000
15000
10000
5000
0
1.00
2.04
1.92
3.83
2.09
10.5
10.0
9.5
9.0
8.5
8.0
7.5
7.0
6.5
6.0
5.5
5.0
4.5
4.0
3.5
3.0
2.5
2.0
1.5
1.0
0.5
0.0
f1 (ppm)

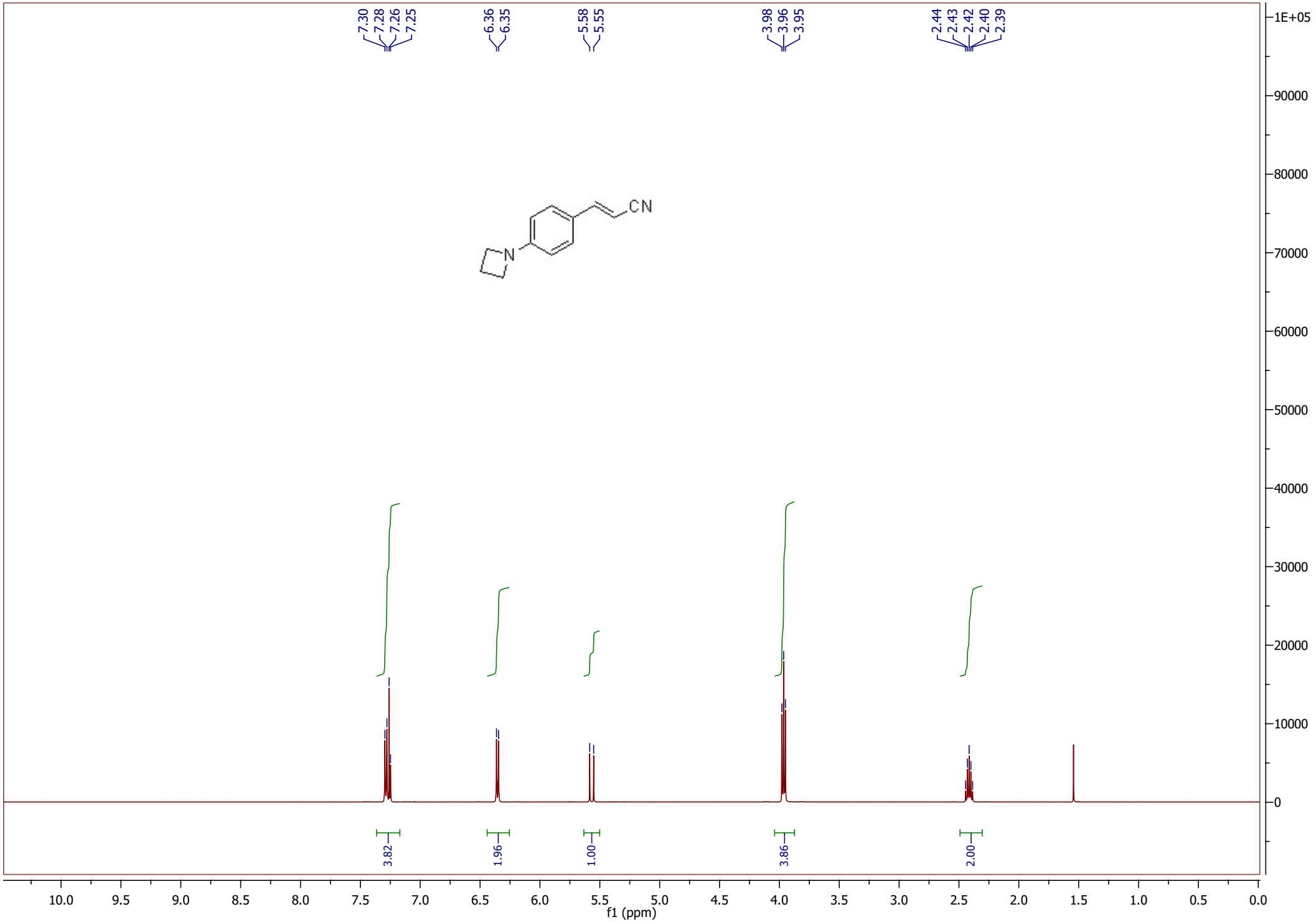
7.30
7.28
7.26
7.25
6.36
6.35
5.58
5.55
3.98
3.96
3.95
2.44
2.43
2.42
2.40
2.39
CN
N
1E+05
90000
80000
70000
60000
50000
40000
30000
20000
10000
0
3.82
1.96
1.00
3.86
2.00
10.0
9.5
9.0
8.5
8.0
7.5
7.0
6.5
6.0
5.5
5.0
4.5
4.0
3.5
3.0
2.5
2.0
1.5
1.0
0.5
0.0
f1 (ppm)

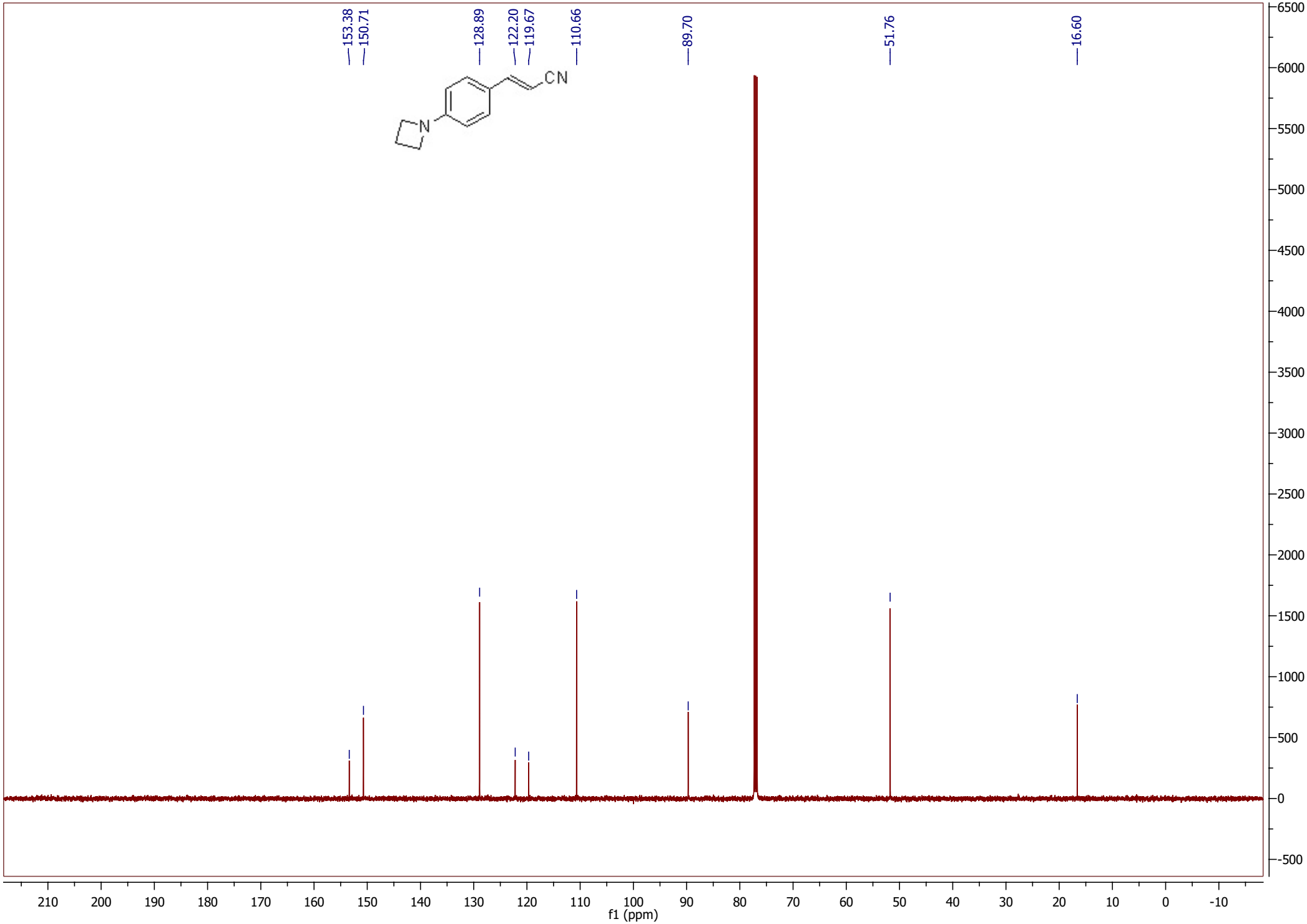
153.38
150.71
128.89
122.20
119.67
110.66
89.70
51.76
16.60
CN
N
6500
6000
5500
5000
4500
4000
3500
3000
2500
2000
1500
1000
500
0
-500
210
200
190
180
170
160
150
140
130
120
110
100
90
80
70
60
50
40
30
20
10
0
-10
f1 (ppm)

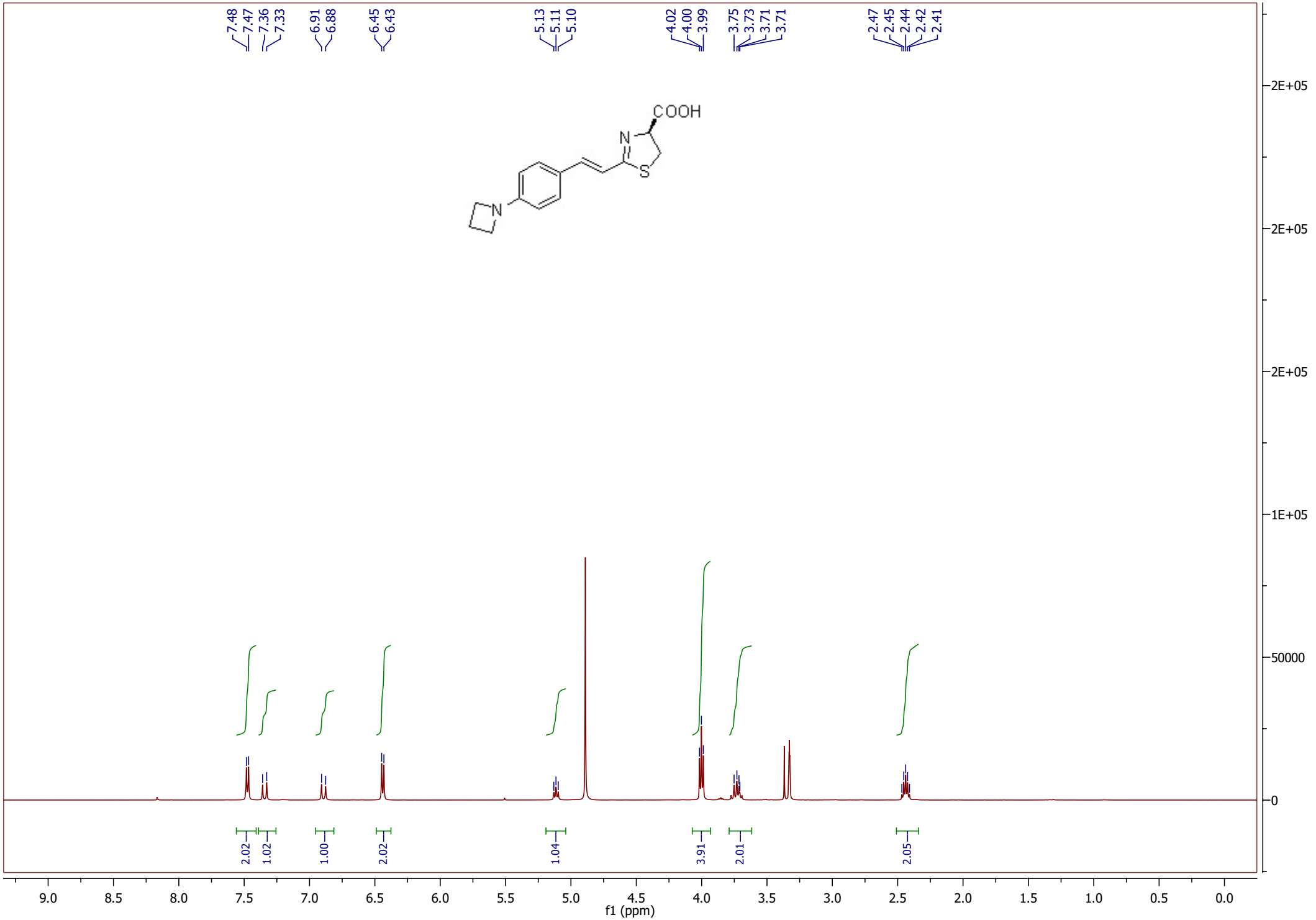
7.48
7.47
7.36
7.33
6.91
6.88
6.45
6.43
5.13
5.11
5.10
4.02
4.00
3.99
3.75
3.73
3.71
3.71
2.47
2.45
2.44
2.42
2.41
COOH
N
S
N
2E+05
2E+05
2E+05
1E+05
50000
0
2.02
1.02
1.00
2.02
1.04
3.91
2.01
2.05
9.0
8.5
8.0
7.5
7.0
6.5
6.0
5.5
5.0
4.5
4.0
3.5
3.0
2.5
2.0
1.5
1.0
0.5
0.0
f1 (ppm)

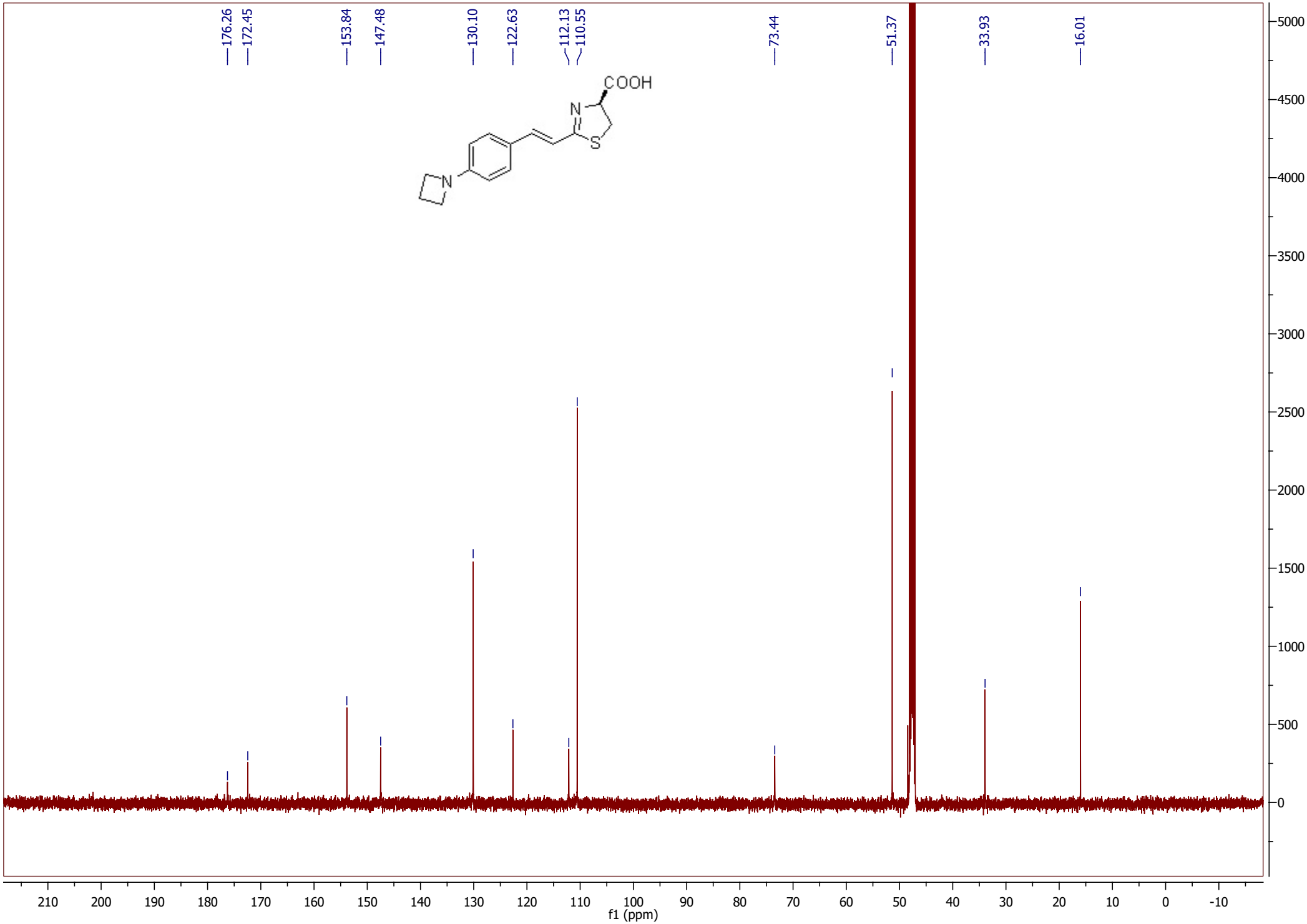
176.26
172.45
153.84
147.48
130.10
122.63
112.13
110.55
73.44
51.37
33.93
16.01
COOH
N
S
N
5000
4500
4000
3500
3000
2500
2000
1500
1000
500
0
210
200
190
180
170
160
150
140
130
120
110
100
90
80
70
60
50
40
30
20
10
0
-10
f1 (ppm)

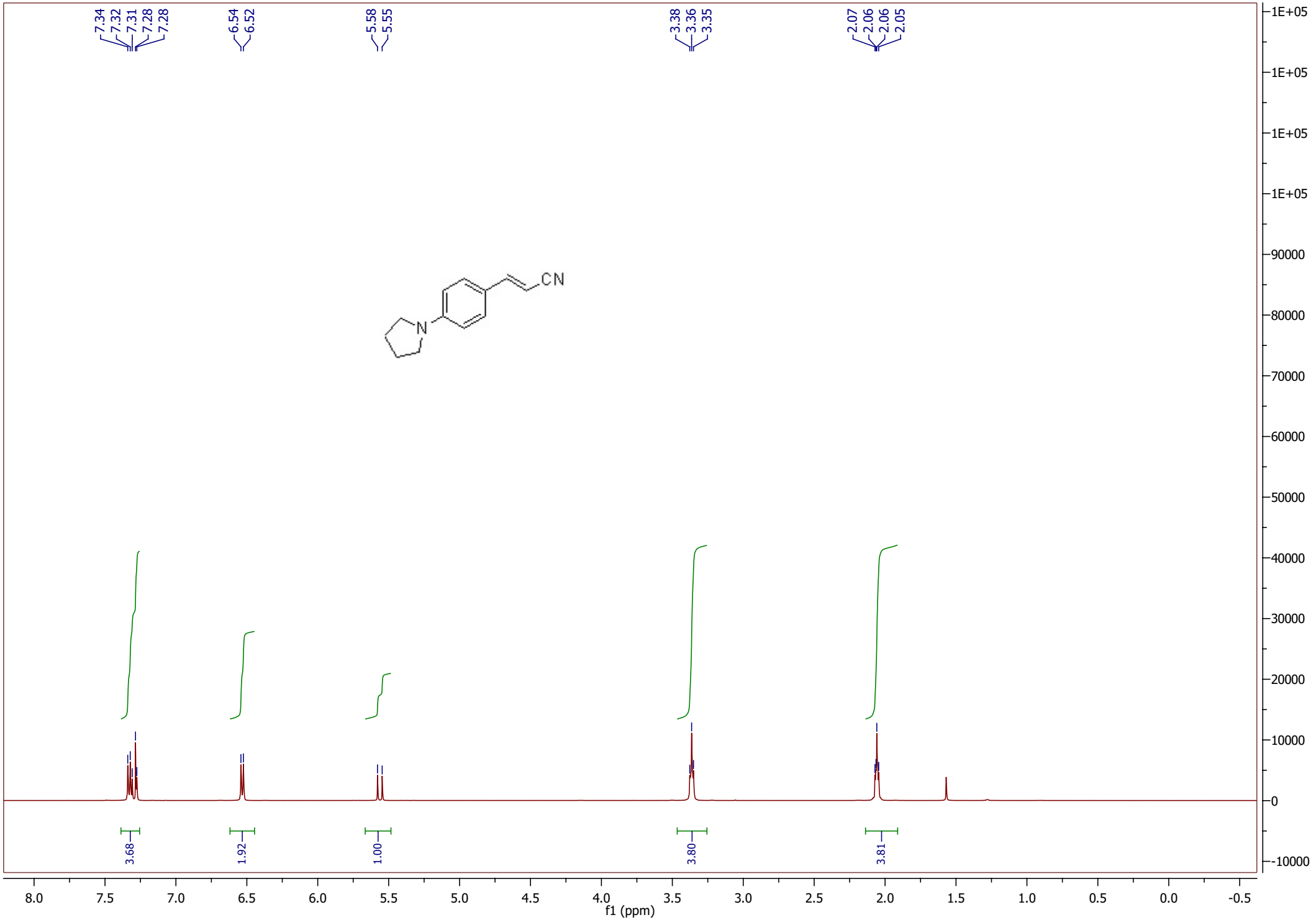
7.34
7.32
7.31
7.28
7.28
6.54
6.52
5.58
5.55
3.38
3.36
3.35
2.07
2.06
2.06
2.05
CN
N
3.68
1.92
1.00
3.80
3.81
1E+05
90000
80000
70000
60000
50000
40000
30000
20000
10000
0
-10000
8.0
7.5
7.0
6.5
6.0
5.5
5.0
4.5
4.0
3.5
3.0
2.5
2.0
1.5
1.0
0.5
0.0
-0.5
f1 (ppm)

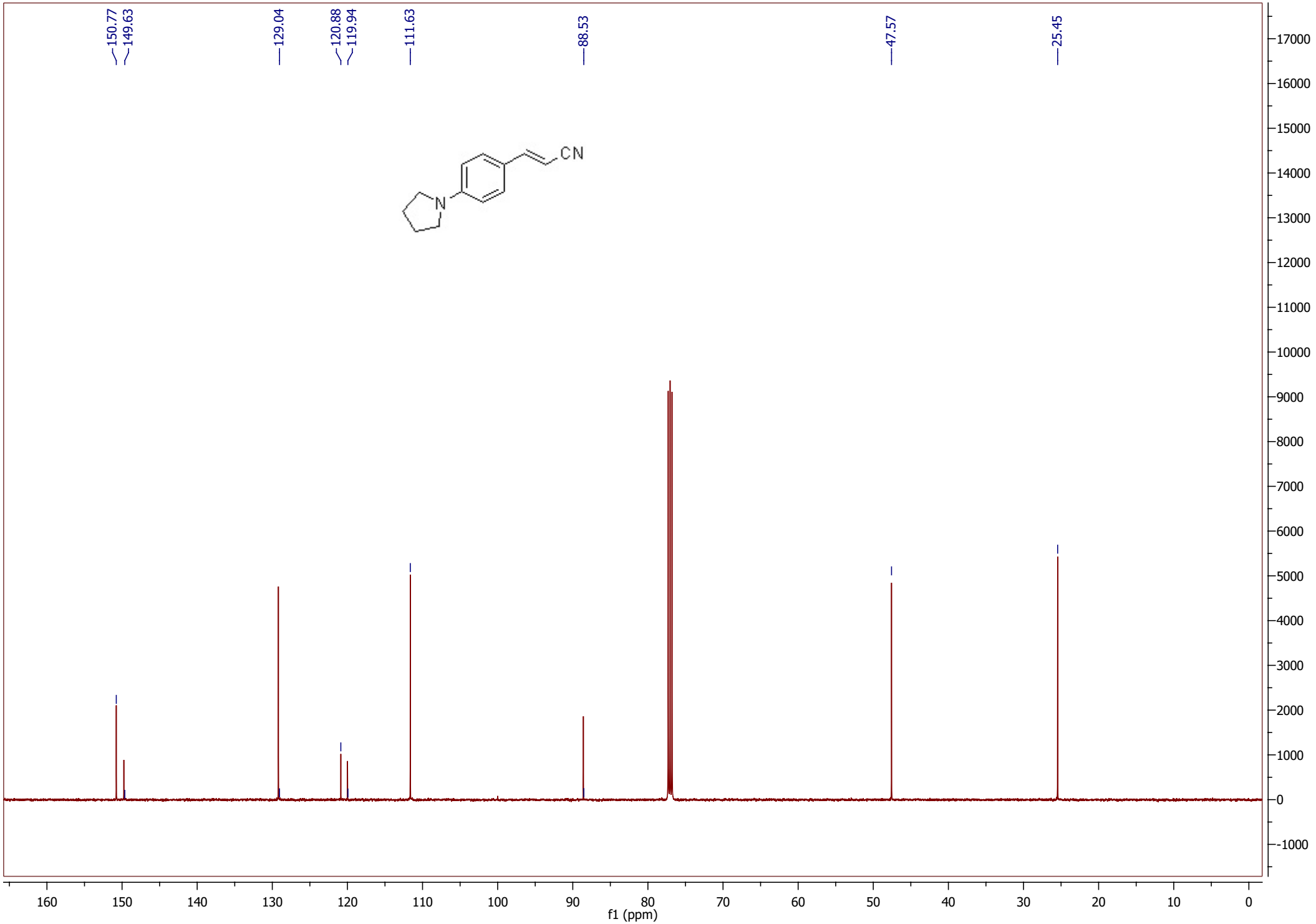
150.77
149.63
129.04
120.88
119.94
111.63
88.53
47.57
25.45
CN
N
17000
16000
15000
14000
13000
12000
11000
10000
9000
8000
7000
6000
5000
4000
3000
2000
1000
0
-1000
160
150
140
130
120
110
100
90
80
70
60
50
40
30
20
10
0
f1 (ppm)

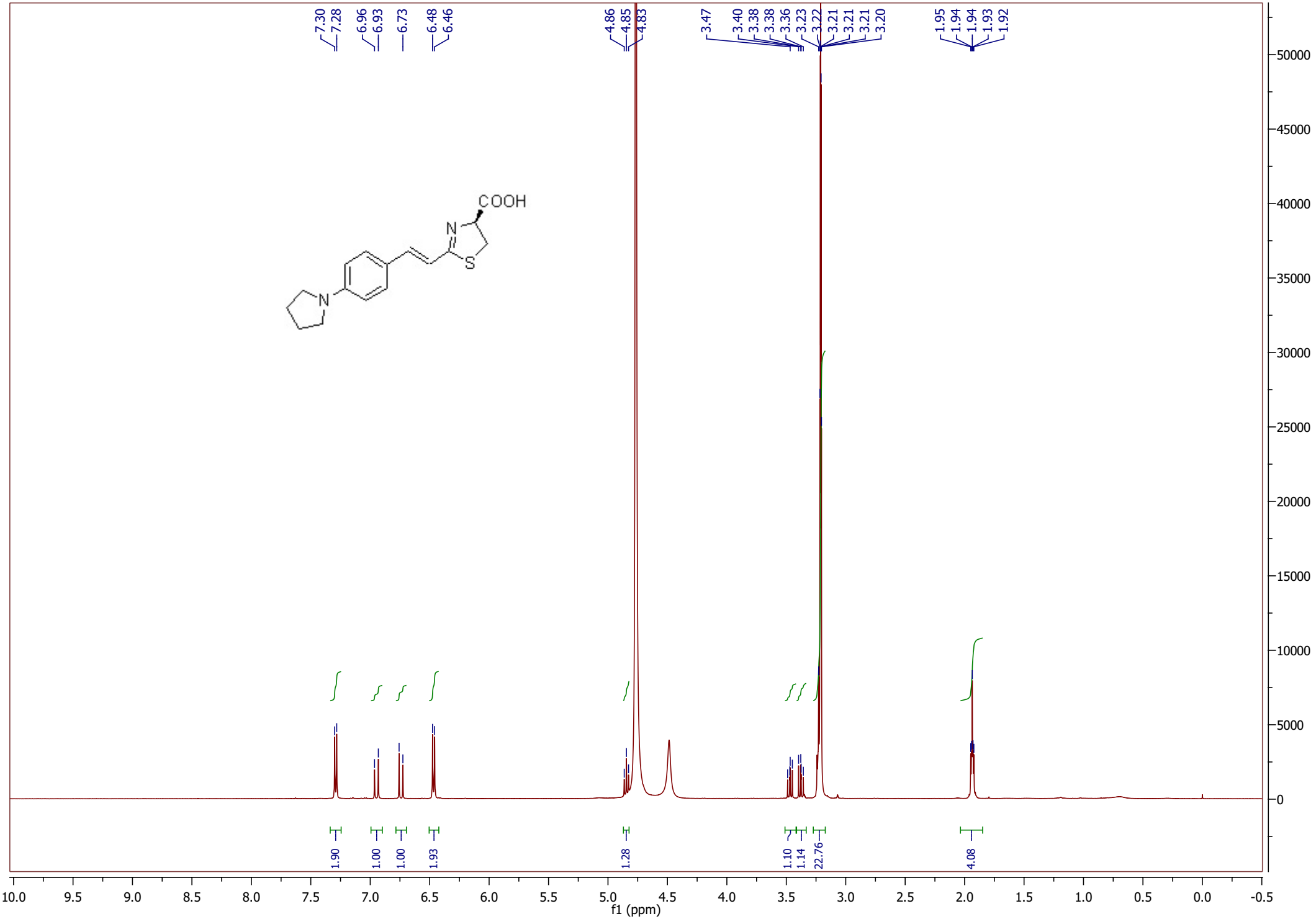
7.30
7.28
6.96
6.93
6.73
6.48
6.46
4.86
4.85
4.83
3.47
3.40
3.38
3.38
3.36
3.23
3.22
3.21
3.21
3.21
3.20
1.95
1.94
1.94
1.93
1.92
COOH
N
S
N
1.90
1.00
1.00
1.93
1.28
1.10
1.14
22.76
4.08
50000
45000
40000
35000
30000
25000
20000
15000
10000
5000
0
10.0
9.5
9.0
8.5
8.0
7.5
7.0
6.5
6.0
5.5
5.0
4.5
4.0
3.5
3.0
2.5
2.0
1.5
1.0
0.5
0.0
-0.5
f1 (ppm)

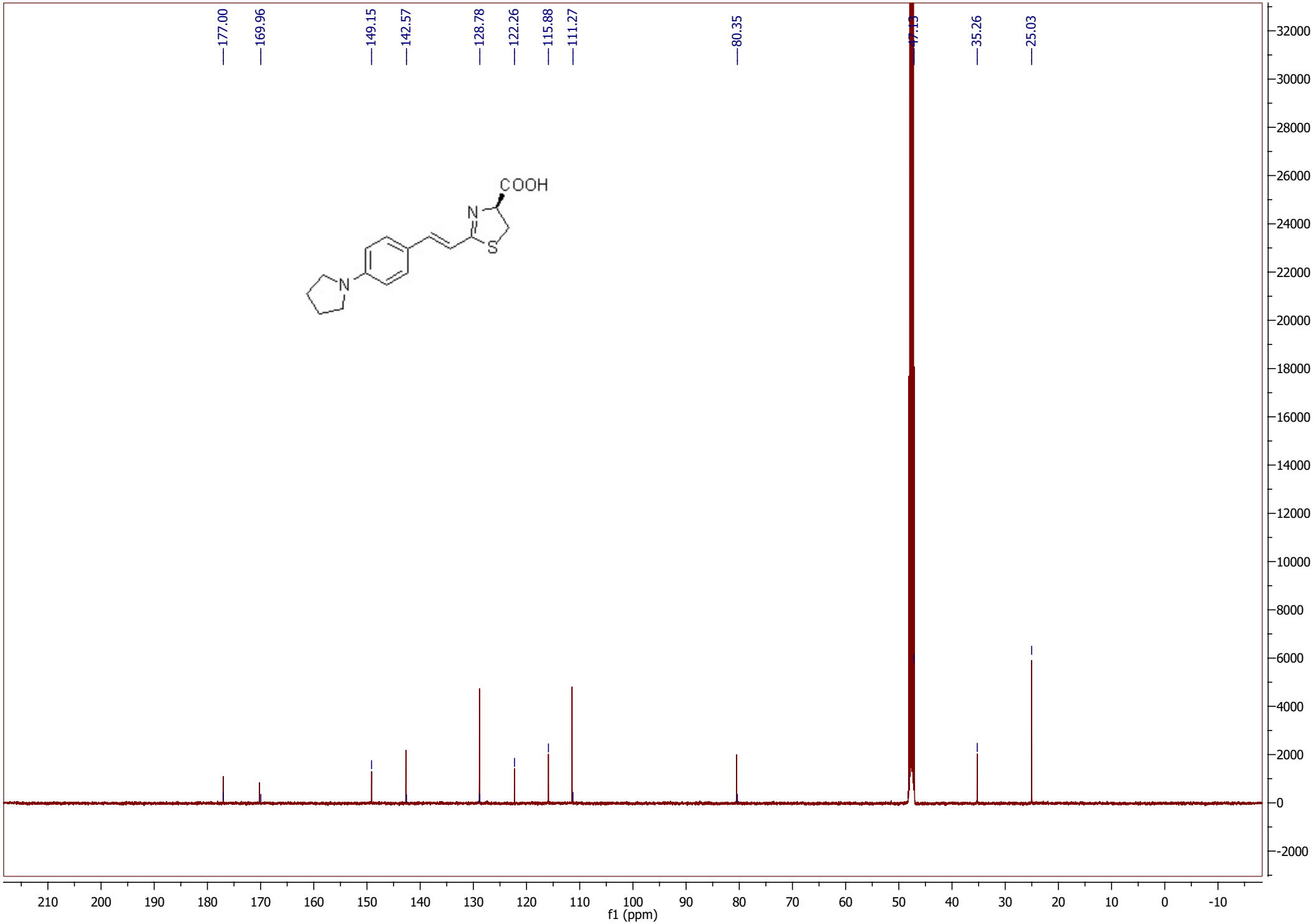
177.00
169.96
149.15
142.57
128.78
122.26
115.88
111.27
80.35
47.13
35.26
25.03
COOH
N
S
N
32000
30000
28000
26000
24000
22000
20000
18000
16000
14000
12000
10000
8000
6000
4000
2000
0
-2000
210
200
190
180
170
160
150
140
130
120
110
100
90
80
70
60
50
40
30
20
10
0
-10
f1 (ppm)